

Correlations of Structure and Rates of Energy Transfer for Through-Bond Energy-Transfer Cassettes

T. G. Kim,[†] J. C. Castro,[‡] A. Loudet,[‡] J. G.-S. Jiao,[‡] R. M. Hochstrasser,[†] K. Burgess,[‡] and M. R. Topp^{*,†}

Department of Chemistry, University of Pennsylvania, Philadelphia, Pennsylvania 19104, and Department of Chemistry, Texas A & M University, P. O. Box 30012, College Station, Texas 77842

Received: June 22, 2005; In Final Form: October 31, 2005

Fluorescent DNA-labeling cassettes are designed to have a common absorbing chromophore matched to a single exciting laser wavelength, but up to four different emitters. Experiments reported here have examined the energy-transfer rates and fluorescence polarization characteristics for two different types of cassette, involving three distinct relative orientations of the donor and acceptor transition moments and the axis of the rigid linker. Energy-transfer times range from <200 fs to ~20 ps, the fastest transfer times occurring when the transition moments of the donor and acceptor species are aligned parallel to the linker axis. Experimental evidence is presented that supports a through-bond energy-transfer mechanism, in contrast with a commercial DNA-labeling agent, which exhibits much slower transfer times controlled by FRET. These rigid cassettes also exhibit polarized fluorescence from the acceptor species, so that this particular type of DNA-labeling probe has some of the advantages of single-molecule probes such as rhodamine and coumarin dyes.

Introduction

A common problem in biotechnology is encountered when several biological molecules labeled with different fluorescent dyes are to be observed by using a single excitation wavelength. A typical example is in DNA sequencing, where termination by fluorescently labeled dideoxy-A, -T, -G, and -C bases must be differentiated.^{1,2} The dye that fluoresces at the shortest wavelength typically has an absorption maximum wavelength, $\lambda_{\text{abs max}}$, close to that of the exciting source, hence it absorbs strongly and emits brightly. Conversely, λ_{max} for absorption by the “red dyes” is not close to the excitation wavelength; those dyes harvest fewer photons and fluoresce relatively weakly. This problem can be partially alleviated by using two dyes arranged to maximize Förster energy transfer (FRET).^{3–6} In that case, a donor dye that absorbs the exciting source strongly couples with an acceptor dye that emits at a longer wavelength. However, the resolution/brightness of such FRET systems is constrained by overlap of the donor emission with the acceptor absorption, corresponding to the overlap integral described in Förster theory.⁷

Our collaboration focuses on donor–acceptor dye cassettes that are connected via a twisted, but otherwise conjugated, π –electron system. The motivation for this is that energy may be transferred through bonds as well as through space. If through-bond energy transfer is the dominant mechanism, then the resolution of multiplexed through-bond energy-transfer cassettes is not constrained by the spectral overlap integral. It should, therefore, be possible to provide brighter and better-resolved systems for multiplexing in biological systems. Through-bond energy transfer has been extensively investigated for development of optical materials,^{8–11} and for photosynthetic models¹² but, prior to our work,^{13–15} not for applications in

biotechnology. Indeed, the types of linkers used in the cassettes described here (diphenylethynyl units) are similar to those employed in work on through-bond energy transfer in porphyrin molecular arrays.¹⁶

The purpose of this paper is to correlate energy-transfer rates and fluorescence polarization characteristics with structure for a range of through-bond energy-transfer cassettes. We believe that the findings of this study may facilitate design of systems to maximize through-bond energy transfer and to retain fluorescence polarization techniques. To do this, we compare the anthracene–BODIPY (BODIPY = 4,4-difluoro-1,3,5,7-tetramethyl-4-bora-3a,4a-diaza-s-indacene) systems **1–9**,¹³ for which some data were reported previously, with the new ¹⁴ fluorescein–rosamine cassettes **10–17**. An important through-space energy-transfer cassette **18** was also studied for comparison.

Cassettes **1–17** have donor and acceptor fragments linked by rigid, π -conjugated systems. They are designed to have common absorbing chromophores matched to the exciting laser, but different emitters. As currently applied in DNA-labeling studies, energy-transfer cassettes employ fluorescein as the common absorber because the absorption maximum of the fluorescein dianion near 490 nm is close to the wavelength(s) of the argon ion laser. Emission is usually from covalently linked rhodamine moieties, the fluorescence of which ranges from 550 to 650 nm. Thus, different DNA bases excited by the same laser can be distinguished via the visible fluorescence of different attached labeling agents.

Usually, energy-transfer cassettes are selected for properties such as distinguishable emission (i.e., relatively narrow band) spectra, high-fluorescence quantum yields, relative ease of attachment to DNA strands, and not least, good photostability. In newer applications of labeling cassettes, which may involve experiments in single-molecule environments such as probe studies of single protein molecules, molecular orientation and fluorescence polarization also become important. That is, an important property of more common molecular probe species,

* Corresponding author. E-mail: mrt@sas.upenn.edu.

[†] Department of Chemistry, University of Pennsylvania.

[‡] Department of Chemistry, Texas A & M University.

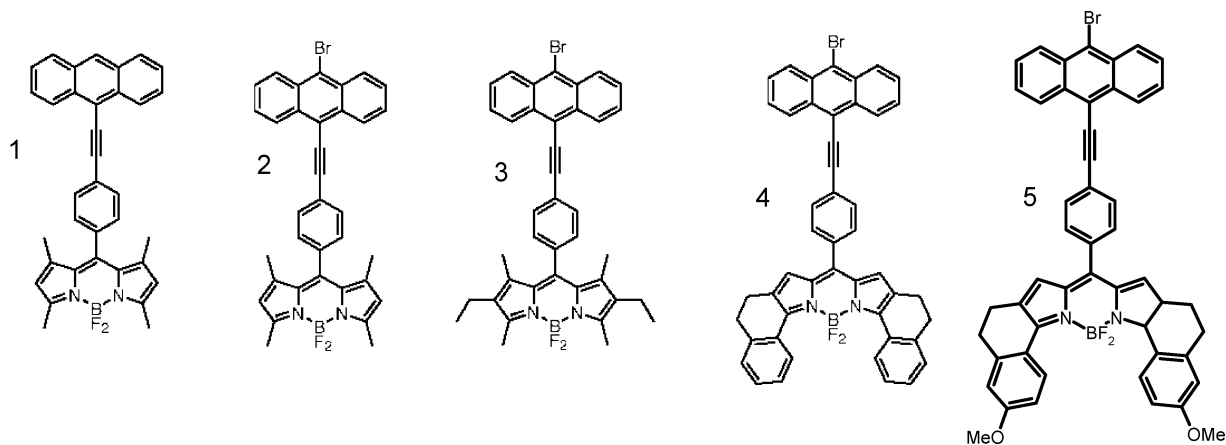


Figure 1. Sequence of anthracene–BODIPY cassettes having perpendicular donor and acceptor transition moments.

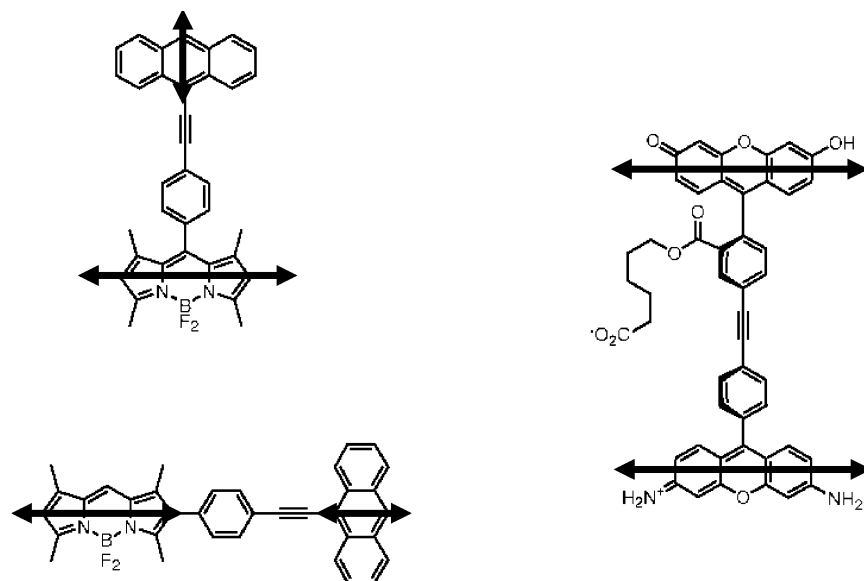


Figure 2. Indications of the directions of the $S_1 \leftarrow S_1$ transition moments in the different energy-transfer cassettes. These are widely quoted, but see refs 19 and 20.

such as rhodamine and coumarin dyes, is that molecular motion and/or orientation can be sensed through time-resolved fluorescence polarization measurements. Similar polarization properties are also desirable in energy-transfer probes, so that structurally rigid probes need to be considered.

The molecules examined in the present study fall into three groups. In the first (Figure 1), compounds **1–5** have a 9- or 9,10-substituted anthracene donor species, excited in our experiments near 405 nm, which transfers energy to a fluorescent BODIPY acceptor moiety. Most of the variation in this sequence involved tuning the emission of the BODIPY emitter via symmetrical structure modification.

The $S_1 \leftrightarrow S_0$ transition moments of the two chromophores are indicated in Figure 2. There, it is seen that compounds **1–5** represent a case where the anthracene $S_1 \leftrightarrow S_0$ transition moment is directed along the axis of the phenylacetylene linker and perpendicular to the transition moment of the BODIPY acceptor. These transition moments are, therefore, mutually perpendicular, independently of the twist angle about the linker axis. Recent work in this laboratory has shown that these species have energy-transfer times in the range 0.42 ± 0.12 ps.¹³

The second set of molecules (compounds **6–9**; Figure 3) uses the same donor and acceptor species, except that the long axis of BODIPY is aligned with the linker. This causes the transition moments (see Figure 2) to be mutually coaxial with the linker,

again, independently of rotation about the linker axis. Also in this set, the length of the linker was varied. Although one purpose of varying the separation of the donor and acceptor moieties was to examine the effects on energy-transfer rates, we found the transfer rate for this set of compounds to be at the lower limit of our instrument response function¹³ (~ 200 fs).

The third set of compounds (**10–17**), shown in Figures 4 and 5, has fluorescein donors, consistent with the commercial applications, and rosamine derivatives as acceptors. (The difference between rhodamine and rosamine lies in the presence or absence of an *o*-carboxyl substituent on the phenyl ring.) Most of the cassettes in the third set, shown in Figure 4, have a diphenylacetylene linker, which maintains the spatial relationship of the donor and acceptor species and, as we show below, gives rise to polarized emission from the acceptor. The energy-transfer times were much longer than those for compounds **1–9**, as shown below. Functionally, compounds **10–17** have in common that the donor and acceptor transition moments are close to mutually parallel, which was confirmed by fluorescence polarization experiments on the donor species and shown below. However, the transition moments are both perpendicular to the axis of the linker, as Figure 2 indicates. A subset of the molecules, shown in Figure 5 (**15–17**), was designed to investigate the effect of varying the linker chain length and type

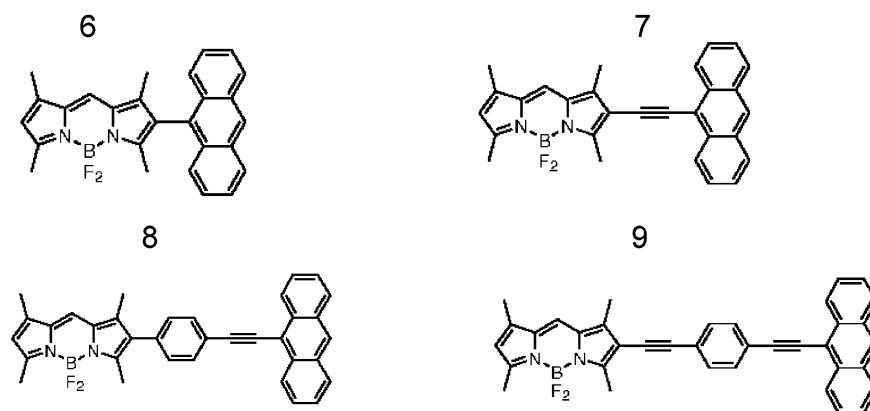


Figure 3. Sequence of anthracene–BODIPY cassettes having parallel donor and acceptor transition moments.

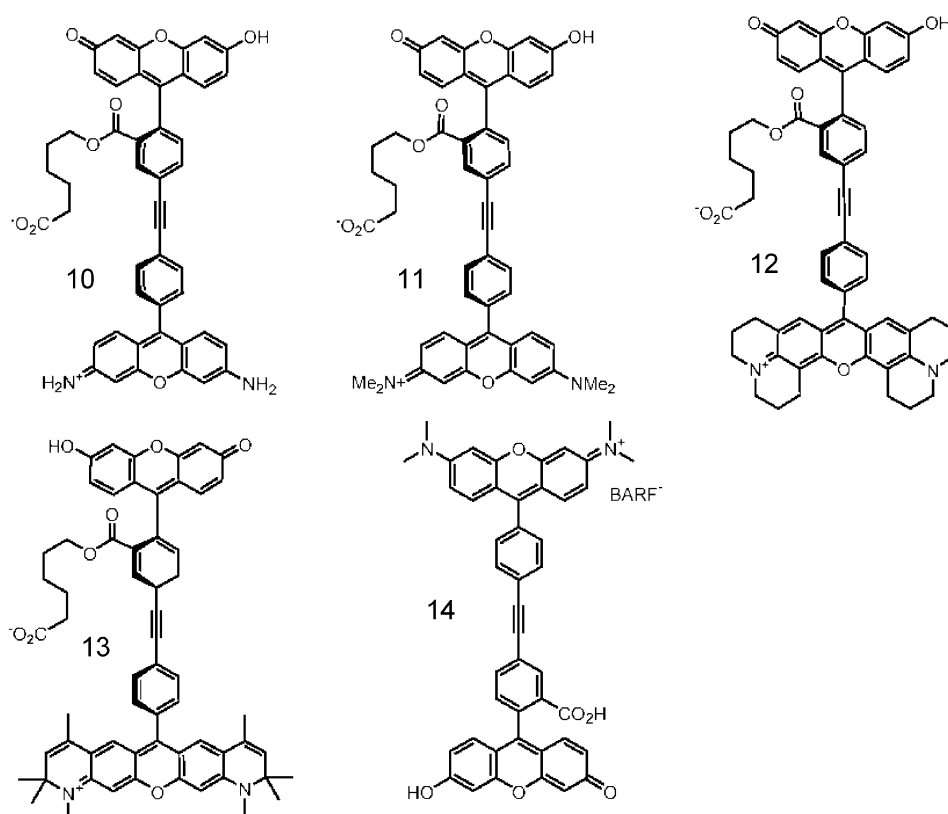


Figure 4. Sequence of fluorescein–rosamine cassettes. All have parallel donor and acceptor transition moments.

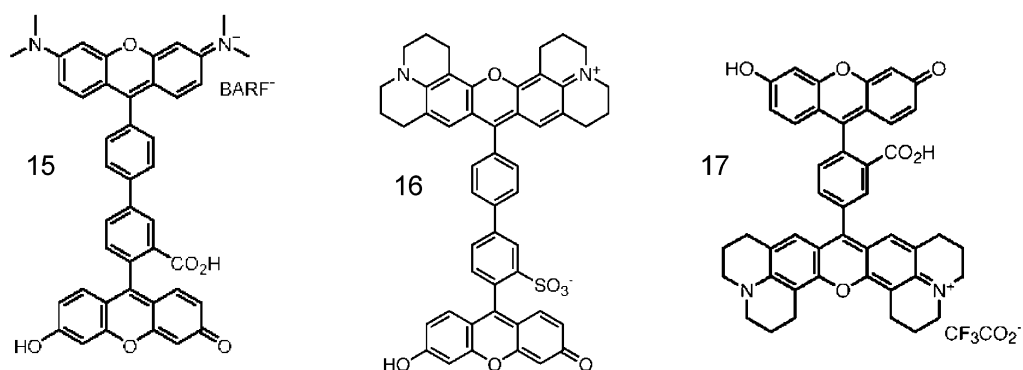


Figure 5. Sequence of fluorescein–rosamine cassettes with shorter linker units. Experiments reported here show that these also have parallel donor and acceptor transition moments.

on two properties of the cassettes: energy-transfer time and polarization anisotropy.

Finally, we compare the above results with a similar measurement on a commercial labeling cassette, “Big-ROX”

(**18**, obtained from ABI), which is shown in Figure 6. Although having almost the same donor and similar acceptor species (rhodamine vs rosamine) to the other cassettes, the two components are unsymmetrically linked by a flexible, partially

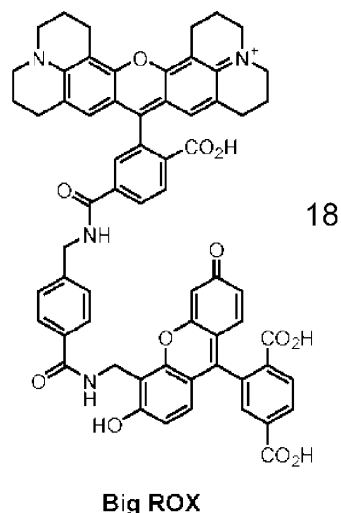


Figure 6. Commercial energy-transfer cassette BIG-ROX, obtained from ABI.

saturated chain. A molecule of this type allows one to examine the dynamical consequences of removing the rigid linker.

Experimental Description

The experiments described here were designed to measure the energy-transfer times of the different cassettes and to examine the fluorescence anisotropy of the donor and acceptor chromophores. The experiments employed ultrafast fluorescence upconversion gating at a time resolution (fwhm) of ≤ 250 fs. Pump-probe studies reported elsewhere¹³ were originally used to study the dynamics of the fastest energy-transfer cases involving detection via $S_{n>1} \leftarrow S_1$ transient absorption of an anthracene donor species in compounds **1–9**, followed by $S_{n>1} \rightarrow S_0$ fluorescence of the anthracene moiety. The present work reports measurements of most of these samples via fluorescence gating methods (see Table 1), which allow verification of the earlier dynamical results and new comparisons of donor and acceptor fluorescence anisotropy. The apparatus incorporated an amplified Ti:sapphire laser delivering femtosecond-domain pulses near 810 nm at a repetition rate near 1 kHz at a power of >200 mW. Most commonly, second harmonic pulses near 405 nm were used for excitation, and detection was carried out near the maximum emission wavelength of both the donor and acceptor species.

For anthracene-based cassettes, 405-nm excitation was sufficient to measure both the population relaxation lifetime and the transient anisotropy. This same wavelength was also sufficient to measure the dynamics of donor relaxation in the fluorescein-rosamine cases (compounds **10–18**), a quantity not found to vary significantly with internal energy. However, anisotropy measurements of compounds **10–18** required excitation near the fluorescein absorption maximum at 490 nm to select an optimally polarized absorption transition. Those experiments used a custom-built noncollinear optical parametric amplifier (NOPA),¹⁷ which was tuned in our experiments over the range 450–530 nm.

Ultrafast fluorescence gating is a now widely established experimental technique and needs little elaboration.¹⁸ Our apparatus (See Figure 7) employed linearly polarized optical pulses, either from the Ti:sapphire second harmonic (near 405 nm) or from the NOPA (450–530 nm), to irradiate the sample contained in a fused silica flow cell of optical path length of ~ 1 mm. A matched pair of off-axis parabolic mirrors collected the emitted fluorescence and refocused it into a 0.5-mm path

TABLE 1: Emission Characteristics of Rigidly Linked Donor-Acceptor Cassettes (Solvent CHCl_3 for Compounds **1–9 and Ethanol for **10–18**, Unless Otherwise Indicated)**

compound no.	acceptor emission maximum (nm)	energy-transfer time (ps)	acceptor emission anisotropy $r(t)^{a,b}$
1	515	0.4	-0.1
2	520	0.49	n/m
3	545	0.55	n/m
4	660	0.33	-0.1
5	690	0.47	-0.09
6	615	<0.2	+0.23
7	650	<0.2	+0.31
8	570	<0.2	n/m
9	590	<0.2	+0.22
10	535	6.0	n/m
11	580	6.8	+0.27
12	605	6.3	+0.25
13	620	5.8; 3.4 (basic EtOH)	+0.20
14	580	~ 6	+0.20
15	575	4.3	+0.19
16	600	2.5	+0.25
17	600	20	+0.20
18	590	35	0

^a Note: The anisotropy $r(t)$ in a fluorescence polarization experiment is defined according to: $r(t) = (I_{\parallel} - I_{\perp}) / (I_{\parallel} + 2I_{\perp})$. If $r(t) = +0.4$, then the absorber and emitter transition moments are parallel; if $r(t) = -0.2$, they are perpendicular. Intermediate values of $r(t)$ from the acceptor suggest some polarization loss during energy transfer. The result $r(t) = 0$ for compound **18** suggests that the donor and acceptor transition moments are uncorrelated. ^b Note: The $r(t)$ values for compounds **1–9** were measured at ~ 2 ps delay after irradiation, those for compounds **10–16** after ~ 10 ps, and that for compound **17** was estimated at ~ 50 ps delay. In all cases, the transient donor anisotropy values were in the range 0.3–0.35, which may indicate an experimental limitation.

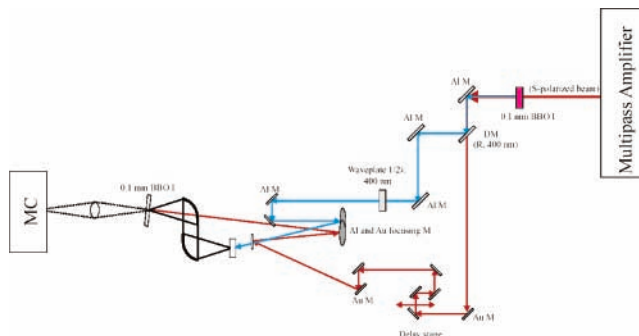


Figure 7. Experimental arrangement for femtosecond-domain fluorescence upconversion experiments.

length BBO crystal. The latter acted as both an optical gate and a polarization selector when irradiated by Ti:sapphire fundamental pulses. The ultraviolet sum-frequency output from the crystal was passed through optical filters into a double monochromator. The signal collected by a photomultiplier was taken to a lock-in amplifier synchronized to the laser pulse rate for noise reduction, and the output fed into a computer. Ultrafast timing employed a computer-controlled optical delay line placed in the path of the gating pulses. The overall time resolution measured by gating either the irradiation pulses or spontaneous Raman scattering was <250 fs, which was sufficient to measure the decay times of most samples in this study.

The tunable NOPA device followed the general features of a design that has been published elsewhere.¹⁷ Briefly, our device was configured as follows (see Figure 8). A small fraction ($\sim 1\%$) of the Ti:sapphire-amplified fundamental beam was focused into a 3-mm sapphire crystal to generate a stable white-

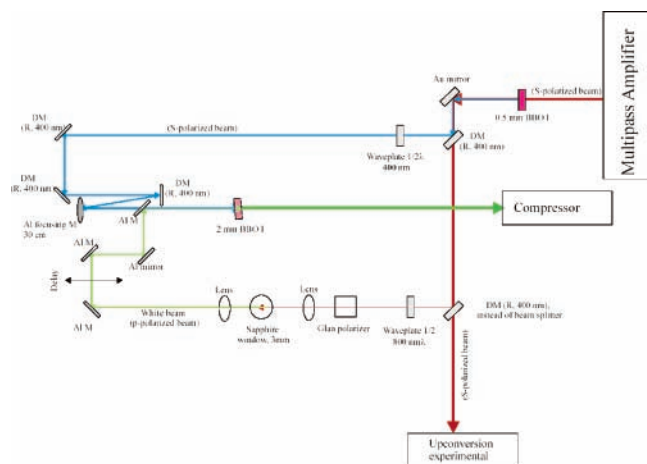


Figure 8. Schematic diagram of the set up for the NOPA tunable femtosecond-domain source.

light continuum, which acted as a “seed” beam for the parametric amplification stage. The emerging continuum pulses were recollimated and taken through an optical delay line before being focused through a 2-mm BBO amplifier crystal. Amplification of part of the continuum was carried out by focusing 405-nm pulses of energy $<50 \mu\text{J}$ (<1 kHz repetition rate) through the BBO crystal. The crystal was displaced from the focus of the 30-cm focusing mirror in order to limit the amplification and thereby stabilize the output. The plane of convergence of the continuum and 405-nm pulses contained the polarization vector of the 405-nm pulses and was perpendicular to the polarization vector of the continuum pulses, in a noncollinear Type-I phase-matched arrangement. Tuning the amplified part of the continuum required accurate synchronization of the pump and the strongly chirped continuum pulses in the crystal, as well as the noncollinear phase-matching angle. The available conversion efficiency was $>20\%$ from the pump pulses, but this was usually scaled back to $\sim 10\%$ for greater stability in optical gating experiments. A pulse compressor was incorporated, to reduce the NOPA pulse durations to <50 fs, allowing us to reduce the effective time resolution of the optical gating device closer to 150 fs. The optimum performance of both the Ti:sapphire laser and the NOPA output was maintained through the use of a CCD spectrometer, which allowed control of the irradiation spectral profiles and center wavelengths. This amount of control allowed us, for example, to monitor gated donor emission at a high signal-to-noise ratio at 525 nm for an excitation wavelength centered at 495 nm. Otherwise, bandwidth fluctuations could cause large amounts of scattered light to enter the signal channel. In addition, the NOPA device allowed us also to tune the excitation to 530 nm to excite the acceptor chromophore in some of the cassettes. Such direct excitation of the acceptor emission provided a means to optimize the anisotropy measurements. Also, direct comparisons of the acceptor anisotropy following excitation of the donor or acceptor moiety allowed us to make useful comparisons of factors affecting the polarization of the acceptor species.

Experimental Results

Relaxation Times. Scanning the gated spectrum at different delay times after the irradiation event produced a sequence of time-resolved emission spectra, which showed a clear decay of the donor emission near 530 nm and a complementary growth of the acceptor emission, peaking to longer wavelengths. Figure 9 gives an example for compound **13**, the data from which show

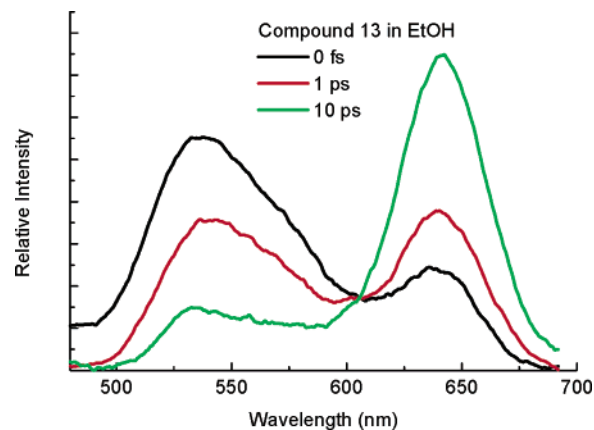


Figure 9. Sequence of gated emission spectra for compound **13** following ultrashort-pulsed excitation at 405 nm.

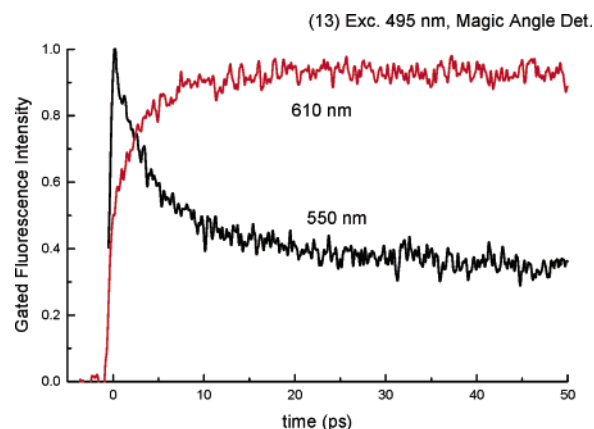


Figure 10. Gated fluorescence time profiles at 550 nm (donor) and 610 nm (acceptor) following ultrashort-pulsed excitation of compound **13** via the NOPA at 495 nm. Magic-angle polarization was used to eliminate transient anisotropy signals.

that the fluorescence spectrum following excitation at 405 nm changes on the time scale of 10 ps from donor emission peaking at 530 nm to acceptor emission peaking at 640 nm. Companion experiments, which involved setting the detector at a particular wavelength while scanning the optical delay, led to time profiles for either the donor or acceptor species. An example is given in Figure 10, also for compound **13**, for which an exponential fit showed the donor signal to decay with a time constant of ~ 5.8 ps. It should also be noted that we excited both fluorescein and rhodamine molecules separately at 405 nm to provide a reference calibration of nonradiative relaxation processes intrinsic to those molecules. A small transient of duration ~ 1 ps was observed for fluorescein, on the short-wavelength edge of the emission spectrum, which may be due to vibrational cooling. An even smaller effect was noticed for rhodamine B. We conclude from these reference experiments that no significant transients due to either the donor or acceptor species alone could account for the temporal evolutions reported here for the energy-transfer cassettes.

The experimental results are summarized in Table 1 for all 18 samples. Samples **1–5** are the anthracene–BODIPY cassettes, where the donor and acceptor transition moments are perpendicular, but the donor transition moment is aligned with the linker axis. These numbers fall close to those reported earlier, being 0.45 ± 0.08 ps. The data for compound **5** are presented here for the first time, the relaxation time being conspicuously longer than that for compound **4**. For the other set of anthracene–BODIPY compounds **6–9**, we found as before that

the transfer times were too fast to measure with this apparatus.

The rest of the data are reported here, for the first time, for compounds **10–18**. Compounds **10–14**, which were designed to have a steady evolution in the donor–acceptor energy gap, show a strikingly similar set of donor relaxation times, in pure ethanol, of 6.2 ± 0.4 ps. For the same set of cassettes, calculations of the Förster integral show a variation of a factor of 2 (see below), suggesting that there should be a similar variation in transfer time, which was not observed.

Compounds **15–17** showed a much greater variation in transfer time, with the most conspicuous difference being for compound **17**. Despite having the shortest linker and parallel transition moments, this showed a relaxation time easily three times longer than for any of the other cassettes noted in Table 1. Another compound similar to **17**, varying only in the anion but not shown here, exhibited almost exactly the same behavior. Clearly, for this cassette, a different, less efficient energy-transfer mechanism was operative.

Finally, compound **18**, the commercial, nonrigid cassette, showed by far the longest transfer time, suggesting that this is limited by FRET. This is distinguished from all other samples, except **17**, by at least a factor of 5.

It should be noted that the energy-transfer times also depended on solvent type, in particular, the presence of water in the ethanol solvent. Thus, pure ethanol solvent prevents deprotonation of the fluorescein donor species, with the result that the oscillator strength is considerably reduced, although the energy of the first excited state is not substantially changed. Even a small amount of water and, especially, the addition of small amounts of base, allowed full deprotonation of the fluorescein, increasing the oscillator strength of the transition. There is a significant difference in the fluorescence quantum yield of isolated fluorescein under these circumstances, but when fluorescein acts as an energy donor in the cassettes, the effect is limited to a factor of 1.7 in energy-transfer rate. Such effects were not explored in further detail, and all of the data presented in Table 1 refer to the pure ethanol case.

Anisotropy Measurements. An important part of these experiments involved measuring the fluorescence anisotropy of both components in these donor–acceptor cassettes. This kind of measurement allows us to correlate the energy-transfer rates between the two chromophores with their relative transition moment orientations. In most cases, the relative orientations are predictable from experience with the isolated fragment fluorescein and rosamine moieties. However, a useful quantity provided by these experiments is the actual amount of anisotropy following energy transfer. Also, for cassettes **15–17**, the relative orientations were not obvious in advance because of a twist induced in the linker.

As Table 1 indicates, anisotropy measurements were made for 14 of the 18 cassettes. The missing data are due to low sample amounts. In any case, all four missing cases were quite similar to others, and so significant data were considered to be lost. Of all the samples studied, only the commercial sample, compound **18**, showed unpolarized acceptor emission despite strong polarization of the donor moiety. We note that, in compound **18**, the donor and acceptor chromophores are linked by a long flexible chain, which is quite different from the rest of the cases shown here.

We have already reviewed the behavior of the anthracene–BODIPY cassettes, for which the sequence **1–5** show perpendicular polarizations and sequence **6–9** show parallel polarizations. We report here for the first time that all of compounds **10–17** also show parallel polarizations. For example, Figure

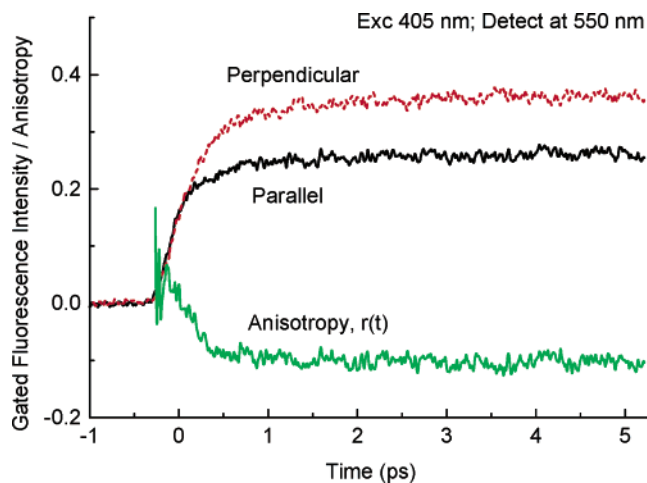


Figure 11. Polarized time profiles of compound **1** in chloroform solvent following 405-nm excitation. Signals monitored at 550 nm, on the acceptor (BODIPY) fluorescence. The negative anisotropy indicates a perpendicular orientation of the donor and acceptor transition moments. For reference, the measured anisotropy of the transient donor emission was +0.33.

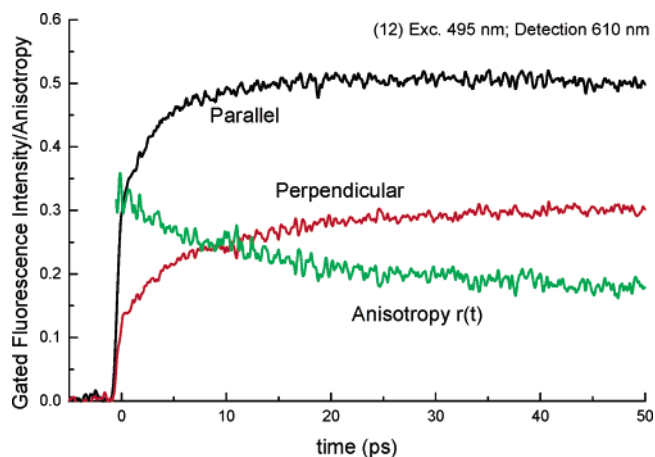


Figure 12. Polarized time profiles of compound **12** in ethanol solvent following 495-nm excitation (donor chromophore). Signals monitored at 610 nm, on the acceptor (rosamine) fluorescence. The fluorescence shows a positive anisotropy, decaying from the vicinity of +0.33 (overlapping donor emission) to near +0.2, indicating a parallel orientation of the transition moments. The $\sim 40\%$ decay in anisotropy over 50 ps indicates some loss of anisotropy during the energy transfer. Approximately half of the overall anisotropy decay is due to molecular motion (see Figure 13).

11 shows the situation for compound **1**. During the rapid transfer process, the anisotropy quickly adopts a value of $r(t)$ near -0.1 , which remains constant during the 5-ps time scale of the scan. Typically, we did not observe ideal values of $r(t)$ (i.e., +0.4 for parallel and -0.2 for perpendicular), possibly due to experimental limitations. Nonetheless, the data are sufficiently definitive to indicate the relative transition moment orientations.

The time profile of compound **12** monitored at 610 nm (Figure 12) shows polarized emission initially from the tail of the donor fluorescence, decaying from 0.32 to ~ 0.20 . Because the relaxation time of the donor emission is ~ 6 – 7 ps, the anisotropy measured >20 ps after irradiation is a property of the acceptor species. The initial decay in the anisotropy, which is direct evidence for the reduced anisotropy of the acceptor emission, could result from a combination of thermally induced excursions of the structure from the strictly parallel orientation of the two transition dipoles. Nonetheless, this result clearly

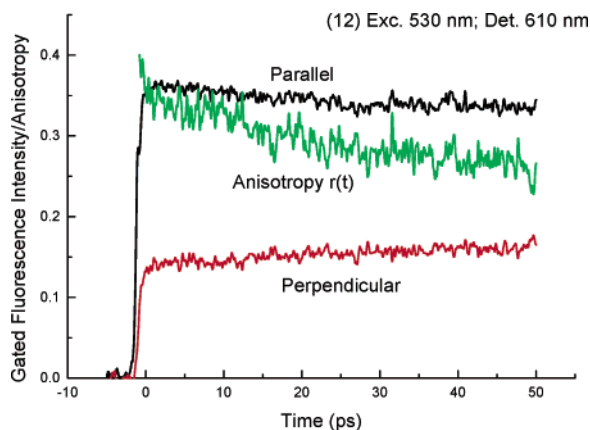


Figure 13. Polarized time profiles of compound **12** in ethanol solvent following 530-nm NOPA excitation of the acceptor chromophore. The anisotropy decays by $\sim 20\%$ over 50 ps due to molecular motion.

shows a substantial polarization of the acceptor emission, which is of considerable potential importance for structural analysis.

For reference, measurements following direct excitation of the acceptor species in compound **12** ($\lambda_{\text{exc}} \sim 530$ nm) (see Figure 13) showed a relatively slow depolarization, consistent with a diffusion-limited relaxation time (by extrapolation) on the order of 150–250 ps. Thus, any time-dependent change in the anisotropy on the time scale < 20 ps, following donor excitation, is due to donor–acceptor energy transfer. The polarization-independent traces, computed from $I_{\parallel}(t) + 2I_{\perp}(t)$, also led to a rising function having a time constant near 7 ps. This was consistent with the direct, magic-angle measurements, which yielded a decay time of 6.3 ps.

We also investigated the dependence of the decay times on solvent conditions, for which we found a factor of 2 decrease in lifetime when some cassettes were dissolved in ethanol solution containing a small amount of aqueous base. This experimental condition ensured deprotonation of the fluorescein group, leading to a maximum absorption cross section at 490 nm due to the fluorescein dianion. Evidently, such deprotonation maximizes the rate of energy transfer.

Energy-Transfer Mechanism. The evidence supports a model for through-bond, as opposed to through-space transfer. A through-space model would involve the nonradiative process of Förster transfer (FRET), which is governed by the equation:¹⁹

$$k_{\text{DA}} = \text{const} \times \frac{k_r^{\text{D}}}{R^6 n^4} \int \kappa^2 \frac{\epsilon_A(\tilde{\nu}) f_{\text{D}}(\tilde{\nu})}{\tilde{\nu}^4} d\tilde{\nu}$$

where the quantity κ , which relates to the orientation dependence of the dipole coupling, is given by:

$$\kappa = (\hat{\mu}_1 \cdot \hat{\mu}_2) - 3(\hat{\mu}_1 \cdot \hat{r}_{12})(\hat{\mu}_2 \cdot \hat{r}_{12})$$

If the transition dipole moments, $\hat{\mu}$, are mutually perpendicular, and if either dipole is perpendicular to the vector, \hat{r}_{12} , linking the centers of the donor and acceptor moieties, then the value of κ will be zero and Förster transfer should not occur. The observation of ultrafast energy transfer (i.e., 300–600 fs) in compounds **1–5**, where this perpendicular condition applies, suggests that Förster transfer is not the prevalent mechanism.

Conclusions

Comparison of the series **1–5** and **10–14** shows no systematic correlation of the transfer rate with the nature of the

acceptor, despite the differences in donor–acceptor energy gap. This also argues against the Förster mechanism, which depends somewhat critically on the overlap integral of the donor emission and acceptor absorption spectra, given by the above equation.

Experiments with cassettes having reduced donor–acceptor distances (**14**, **15**, **17**) also showed no significant increase in transfer rates, as would be predicted from Förster theory. On the contrary, results obtained for compound **17** showed that, when the linker is reduced to a single carboxylated phenyl group, the transfer rate is much reduced. This indicates a significant reduction in the amount of coupling of the two chromophores, despite their continued parallel arrangement, which is currently unexplained. Similar variation of the donor–acceptor transfer distances in compounds **6–9** also did not reveal any correlations between the rates and the separation. In those cases, the transfer rates were faster than our experiments could reliably resolve (i.e., more than $30\times$ faster than that for the similar fluorescein–rhodamine cases) and, again, not predicted by Förster theory. We note here that the donor and acceptor transition moments are both aligned with the linker axis, which is the case that clearly optimizes the transfer rates.

Fragment compounds were also synthesized, such as a fluorescein type of donor and several acceptors of the type seen in cassettes **10–14**. Calculations of the spectral overlap integrals between a given donor and several different acceptors show a variation of up to a factor of > 2 for different cassettes, the maximum overlap being achieved for cassette **11**. If Förster transfer were significant, one would expect a similar variation in the transfer rates, which was not actually observed. Also, given the r^{-6} dependence of the Förster integral, one could expect a strong dependence on the separation of the two chromophores, which again, we do not see. Therefore, we conclude that Förster transfer is unlikely to represent the main mechanism for energy transfer in most of the cassettes shown here. Of all the synthetic cassettes in this study, just one, compound **17**, shows a slow energy transfer more consistent with a Förster type of mechanism.

The decay times of **15** and **16** were somewhat shorter than those of **10–14**, but within the variation we have observed in different solvents. Also, fluorescence polarization measurements clearly showed that the transition moment of the acceptor rosamine species remained parallel to that of the donor, indicating a canceling twist induced by the biphenyl linker. The surprise was with compound **17** (and a similar compound not shown here), where the energy-transfer time increased to around 20 ps (i.e., nearly an order of magnitude slower than **15** and **16**). Note that, in compound **17**, the donor–acceptor separation is the closest for this entire family of molecules (**10–17**), and the polarization experiments again showed that the transition moments remain parallel. Despite the reduction in the physical distance between the chromophores, the coupling is significantly weaker. This behavior is consistent with through-bond energy transfer, which is influenced by the nature of the linker bonds intermediate between the donor and acceptor moieties.^{16,20}

Finally, compound **18**, the commercial sample “Big-ROX”, which contains flexibly linked fluorescein and rhodamine chromophores, shows a relaxation time nearly an order of magnitude longer than that for the other cassettes **10–16**. This is a case that more clearly reflects through-space (FRET) as opposed to through-bond transfer. This is different behavior from compound **17**, which also shows slow energy transfer, but both the donor and acceptor emissions are polarized.

Acknowledgment. This research was supported by grants NIH5-P41-RR001348 (to R.M.H.) and NIH GM72041, HG01745, and the Robert Welch Foundation (to K.B.).

References and Notes

- (1) Hood, L. E.; Hunkapiller, M. W.; Smith, L. M. *Genomics* **1987**, *1*, 201–212.
- (2) Smith, L. M.; Sanders, J. Z.; Kaiser, R. J.; Hughes, P.; Dodd, C.; Connell, C. R.; Heiner, C.; Kent, S. B.; Hood, L. E. *Nature (London)* **2004**, *321*, 674–679.
- (3) Ju, J.; Kheterpal, I.; Scherer, J. R.; Ruan, C.; Fuller, C. W.; Glazer, A. N.; Mathies, R. A. *Anal. Biochem.* **1995**, *231*, 131–140.
- (4) Ju, J.; Ruan, C.; Fuller, C. W.; Glazer, A. N.; Mathies, R. A. *Proc. Natl. Acad. Sci. U.S.A.* **1995**, *92*, 4347–4351.
- (5) Ju, J.; Glazer, A. N.; Mathies, R. A. *Nat. Med.* **1996**, *2*, 246–249.
- (6) Nampalli, S.; Khot, M.; Kumar, S. *Tetrahedron Lett.* **2000**, *41*, 8867–8871.
- (7) Lakowicz, J. R. *Principles of Fluorescence Spectroscopy*, 2nd ed.; Kluwer Academic/Plenum: New York, 1999.
- (8) Weder, C.; Wrighton, M. S. *Macromolecules* **1996**, *29*, 5157–5165.
- (9) Swager, T. M.; Gil, C. J.; Wrighton, M. S. *J. Phys. Chem.* **1995**, *99*, 4886–4893.
- (10) McQuade, D. T.; Pullen, A. E.; Swager, T. M. *Chem. Rev.* **2000**, *100*, 2537–2574.
- (11) Tour, J. M. *Chem. Rev.* **1996**, *96*, 537–553.
- (12) Holten, D.; Bocian, D.; Lindsey, J. S. *Acc. Chem. Res.* **2002**, *35*, 57–69.
- (13) Wan, C.-W.; Burghardt, A.; Chen, J.; Bergström, F.; Johansson, L. B.-Å.; Wolford, M. F.; Kim, T. G.; Topp, M. R.; Hochstrasser, R. M.; Burgess, K. *Chem.—Eur. J.* **2003**, *9*, 4430–4441.
- (14) Jiao, G.-S.; Thoresen, L. H.; Burgess, K. *J. Am. Chem. Soc.* **2003**, *125*, 14668–14669.
- (15) Burghardt, A.; Thoresen, L. H.; Chen, J.; Burgess, K.; Bergström, F.; Johansson, L. B. A. *Chem. Commun.* **2000**, 2203–2204.
- (16) Holten, D.; Bocian, D. F.; Lindsey, J. S. *Acc. Chem. Res.* **2002**, *35*, 57–69.
- (17) Wilhelm, T.; Piel, J.; Riedle, E. *Opt. Lett.* **1997**, *22*, 1494–1496.
- (18) Baskin, J. S.; Yu, H. Z.; Zewail, A. H. *J. Phys. Chem. A* **2002**, *106*, 9837–9844.
- (19) Kleima, F. J.; Hofmann, E.; Gobets, B.; van Stokkum, I. H. M.; van Grondelle, R.; Diederichs, K.; van Amerongen, H. *Biophys. J.* **2000**, *78*, 344–353.
- (20) Speiser, S. *Chem. Rev.* **1996**, *96*, 1953–1976.